ELSEVIER

International Journal of Pharmaceutics 120 (1995) 235–245

international journal of pharmaceutics

Solid-state transformation of a leukotriene antagonist

C.S. Randall [a,*], B.K. DiNenno [a], R.K. Schultz [b], L. Dayter [c], M. Konieczny [c], S.L. Wunder [c]

[a] *SmithKline Beecham Pharmaceuticals, P.O. Box 1539, King of Prussia, PA 19406, USA*
[b] *3M Health Care, St. Paul, MN, USA*
[c] *Department of Chemistry, Temple University, Philadelphia, PA, USA*

Received 10 November 1993; revised 29 September 1994; accepted 6 December 1994

Abstract

SK&F 104353, a potent leukotriene antagonist, exists in two physically distinct species as a disodium salt. Type I melts with decomposition, showing a single endotherm in the region of 250–270° C in differential scanning calorimetry (DSC) thermograms, as well as exhibiting a weak powder X-ray diffraction (XRD) pattern. Type II contains a single DSC melting endotherm in the same region, but in contrast has additional, smaller endotherms in the region of 70–85° C; the new transitions remain upon cooling and reheating. The powder XRD pattern of II is very similar to that of I with respect to peak positions, but II's bands are sharper, suggestive of increased crystallinity. Types I and II can also be distinguished using solution calorimetry, manifesting different heats of solution in an ethanol/water mixture. Apparent irreversible conversion of I to II can readily occur, and has a significant impact with respect to physical stability of potential suspension aerosol formulations. The results are explained in terms of a solid-state transformation, i.e., from a metastable, partially amorphous form of low crystallinity (I) to a similar but more physically stable form of higher crystallinity (II); the conversion is facilitated by the presence of water, although true 'hydration' is not involved. Temperature-dependent Raman spectroscopy has been applied to characterize the transformation in more detail. The unusual solid-state behavior of this compound may reflect more general structural characteristics of leukotriene antagonists.

Keywords: Leukotriene antagonist; Calorimetry; Powder X-ray diffraction; Raman spectroscopy; Microscopy; SK&F 104353; SK&F 103944

1. Introduction

2(*S*)-Hydroxy-3(*R*)-[2-carboxyethyl)thiol-3-[2-(phenyloctyl)phenyl]propionic acid (SK & F 104353) is a potent and selective peptidoleukotriene receptor antagonist which has potential applications for treatment of asthma and other pulmonary diseases (Gleason et al., 1987; Robuschi et al., 1992). The free dicarboxylic acid form (Fig. 1) is isolated as a water-insoluble oil; efforts have thus focused on identifying suitable salts for formulation development. The disodium salt, SK&F 104353-Z_2, is of particular interest with respect to its physical properties, existing as

* Corresponding author.

0378-5173/95/$09.50
SSDI 0378-5173(95)00004-6

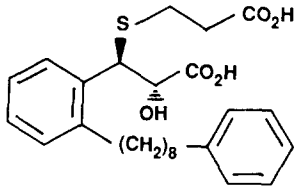

Fig. 1. Structure of SK&F 104353.

two distinct species. Type I, the synthetic product typically obtained by precipitation from absolute ethanol, appears to be a metastable form of low crystallinity. Exposure of I to moisture, e.g., by storage of drug substance under high relative humidity conditions, results in transformation to a more physically stable form of higher crystallinity, type II. The conversion of I to II can be followed by XRD, DSC, optical microscopy, and solution calorimetry. The conversion has been further examined as a function of temperature using Raman spectroscopy; the functional groups most affected appear to be the methylene groups in the hydrocarbon chain regions. The implications of the existence of different physical types of the drug substance are discussed with respect to synthetic process control and suspension aerosol formulation.

2. Materials and methods

2.1. Synthesis

Preparation of SK&F 104353 free acid has been reported (Gleason et al., 1987, Flisak et al., 1993). The disodium salt form was obtained by adding 0.56 N sodium hydroxide/ethanol solution (98.8% EtOH, v/v) to SK&F 104353 previously dissolved in absolute ethanol, at a constant rate with stirring, until a final pH of 8.2–8.5 was reached. The precipitated solid was filtered, washed repeatedly with absolute ethanol, and dried at 65° C under vacuum for several hours, resulting in a white to off-white powder that is highly water soluble, > 100 mg/ml.

Chemical stability of samples was evaluated by reversed-phase high performance chromatography (HPLC) using a C-18 column and a mobile phase consisting of acetonitrile/water/trifluoroacetic acid (65:35:0.1) with a flow rate of 2.0 ml/min.

Residual moisture was determined by coulometric Karl Fischer titration using a Mitsubushi moisturemeter, model CA-05.

2.2. DSC

Thermograms were recorded using a Perkin-Elmer DSC-7 scanning calorimeter equipped with a thermal analysis data system (Perkin-Elmer, Norwalk, CT). Unless otherwise noted, samples were lightly crimped in standard aluminum pans, i.e., closed, but not hermetically sealed, and heated at a rate of 20° C/min.

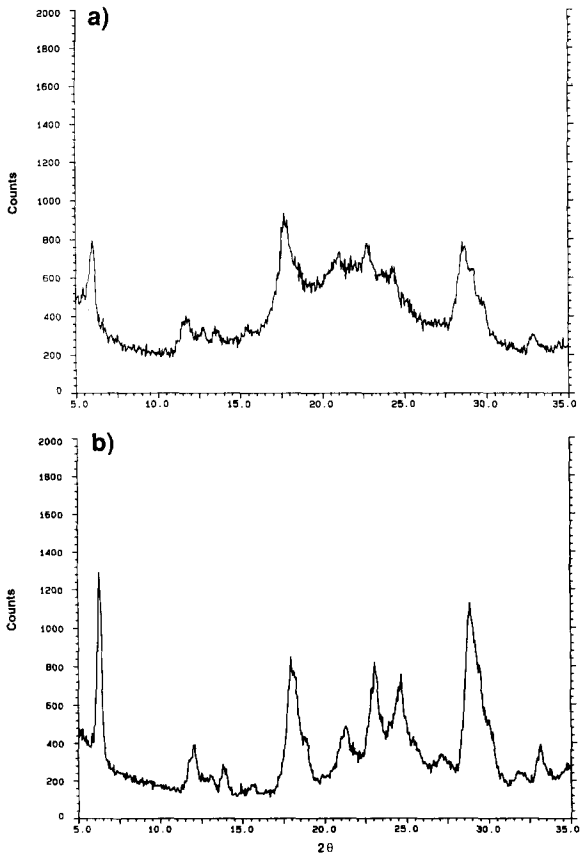

Fig. 2. XRD patterns of SK&F 104353-Z_2: (a) type I drug substance; (b) type II, produced by treating type I with 50:50 ethanol/water. Similar effects were observed when type I drug substance was stored at high humidity.

2.3. XRD

Powder diffractograms were obtained using a General Electric XRD-5 diffractometer with a Siemens automation system (Siemens Analytical X-Ray, Madison, WI). Samples were lightly ground, then slurried with a 1% solution of collodion in amyl acetate. The slurry was layered on a silica single crystal substrate and air dried.

2.4. Solution calorimetry

Heats of solution at 25° C were measured with a Tronac Model 450 isoperibol calorimeter (Tronac, Orem, UT). The principles and experimental design of this system have been described elsewhere (Lindenbaum and McGraw, 1985). Sample amounts on the order of 40–60 mg were accurately weighed into soft glass ampoules. The

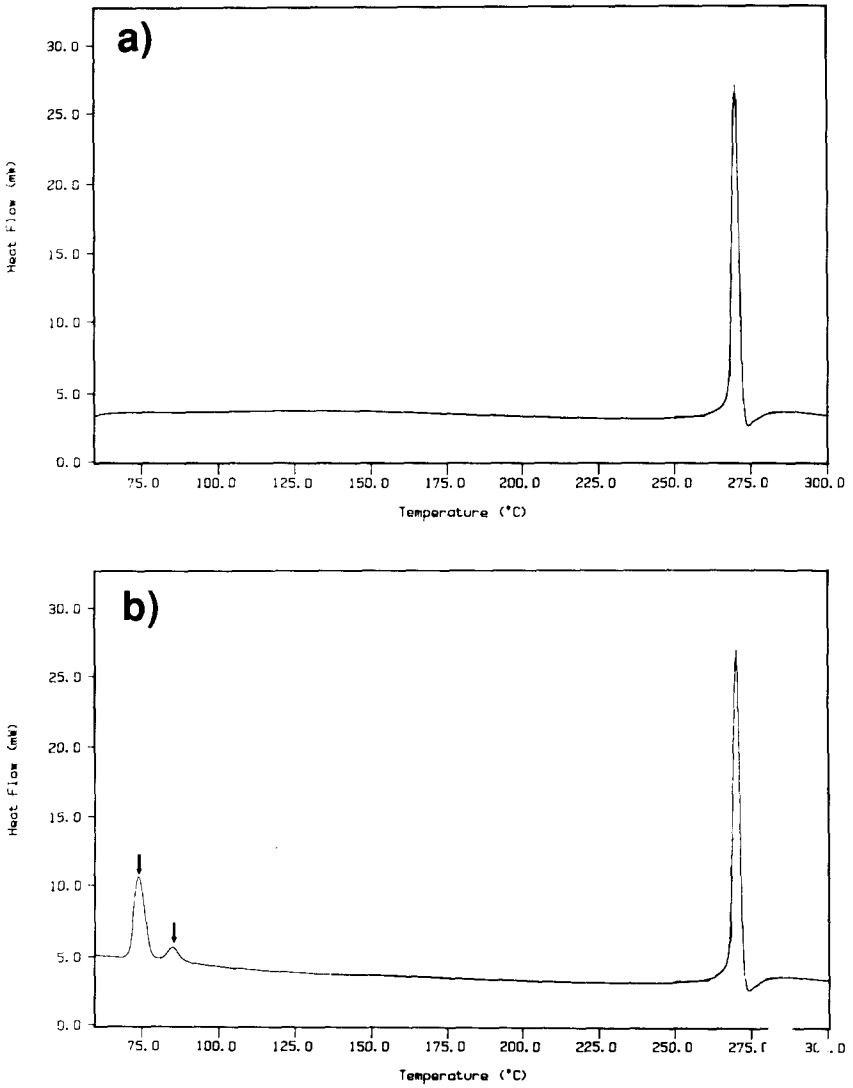

Fig. 3. DSC thermograms of SK&F 104353-Z_2: (a) type I; (b) type II.

solvent system chosen was a 50:50 mixture of ethanol/water, wherein SK&F 104353-Z_2 readily dissolves, producing a measurable heat of solution.

2.5. Microscopy

The particle size and shape of the unconverted drug substance were evaluated by dispersing a small amount of the powder into a test tube containing approx. 3 ml of an inert fluorocarbon liquid (Fluorinert, FC-80, 3M, St. Paul, MN) using a small metal spatula to blend the powder with the liquid. A drop of the resulting dispersion was placed onto a glass microscope slide and observed at 400 × power using a Nikon Biophot light microscope equipped with plan apochromatic objectives and a 35 mm SLR camera (Nikon Inc., Garden City, NY). To prepare the converted drug substance, a small amount of unconverted SK&F 104353-Z_2 was placed in a glass test tube, to which a 50:50 ethanol-water mixture was added dropwise until a slurry developed. After 2–3 min, a drop of the slurry was placed on a glass microscope slide and observed as above. The morphology and particle size of the drug particles in suspension aerosol formulations were evaluated as follows: the metered dose inhaler (MDI) canister was shaken and actuated twice through a plastic actuator in order to prime the valve. The MDI was removed from the actuator, and the valve was actuated directly onto a glass slide; the particles from the captured spray were observed microscopically at 400 × power.

2.6. Raman

Raman spectra were obtained using a SPEX Micramate 1403 double monochromator (SPEX, Edison, NJ) with 1800 grooves/mm holographic gratings. Slit widths of 500 mm, corresponding to 5 cm^{-1} resolution, were used since spectra taken at 2 cm^{-1} resolution yielded identical results. Samples were illuminated with approx. 30 mW of of 514.5 nm radiation from a Coherent model no. 90-5 argon ion laser (Coherent, Palo Alto, CA). Temperature-dependent spectra were obtained using a Linkam Model THM 600 RTD temperature controlled hot stage (Linkam, Tadworth, UK) which fitted between the microscope objective and the microscope stage. In order to record the true sample temperature, the sample was placed directly on a separate copper constantan thermocouple inside the hot stage.

3. Results and discussion

The XRD patterns of types I and II are shown in Fig. 2. The similarity in peak positions suggests that they have the same crystal structure, but

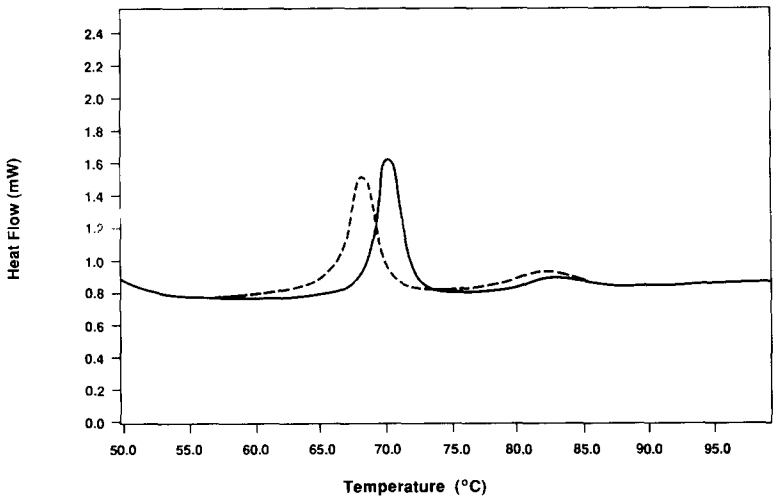

Fig. 4. Expanded DSC region of type II: (solid line) initial heating to 100° C; (broken line) re-heating, after cooling same sample to room temperature.

differ in extent of crystallinity. Type I's powder pattern is characteristically weak and diffuse; however, there are indications of long range order suggesting it is not a truly 'amorphous' material. Type II's pattern is significantly sharper, consistent with an increase in crystallinity and stronger long-range order.

The XRD results correlate well with their respective DSC thermograms (Fig. 3). Both forms exhibit melting with concomitant decomposition above 250° C. The decomposition process causes some uncertainty in determining the true onset of melting as well as an accurate enthalpy of melting; a typical value for the latter is on the order of 120 J/g. This value is considerably below what would be expected for the melt of a highly crystalline material. As expected, reheating of samples that had undergone melting gave thermograms devoid of any thermal events. In contrast to type I, the initial thermogram of type II exhibits melting at approx. 250° C plus two additional, smaller endotherms, at approx. 71 and 85° C, which are well below the region of melting/decomposition. The new endotherms are relatively small (the more prominent 71° C endotherm has a typical enthalpy of 22 J/g), but reproducible; note that they are still present upon cooling and reheating to 100° C, albeit slightly shifted to lower temperature (Fig. 4). The effects of varying the DSC heating rate on these transitions were also studied. Slower heating rates decreased the onset temperatures of the new type II transitions, but the effect was slight and their appearance was otherwise unchanged. These endotherms are also present when a type II sample is heated in an open DSC pan, as well as in a sealed one, indicating that they are not artifacts produced by crimping.

TGA studies were also carried out on type I and type II samples exposed to different relative humidities. The objective of such studies was to assess whether hydrate formation exists in type II. A representative TGA thermogram is shown in Fig. 5b, and a compilation of TGA weight loss as a function of humidity and storage time is given in Table 1. While the drug substance does acquire some moisture at high humidity, there is no indication of hydrate formation. Rather, the

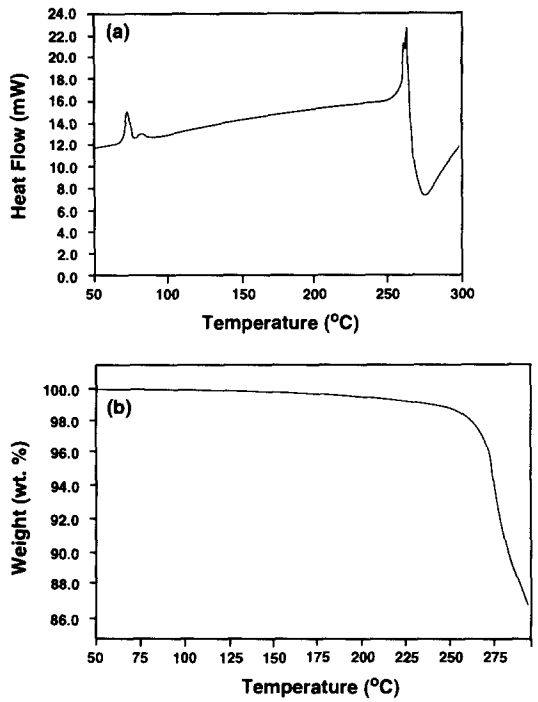

Fig. 5. Comparison of DSC and TGA data for type II: (a) DSC; (b) TGA. Type II was produced by spiking type I with 5% water by weight, then storing in a desiccator with Drierite.

water that is taken up by the drug substance appears to be surface adsorbed, and can be easily driven off in the presence of a drying agent, or by mild heating. The lack of correlation between the DSC and TGA data for type II (Fig. 5) argues against formation of a stable hydrate species.

To rule out chemical degradation as a factor in the conversion, both forms were assayed by

Table 1
Hygroscopicity study of SK&F 104353-Z_2

Condition	Average percent weight loss (TGA)						
	Days						24 h desiccator [b]
Initial [a]	0.51	1	2	3	4	7	
32% R.H.		0.74	0.80	0.66	0.53	0.64	
58% R.H.		0.98	0.98	0.86	0.98	1.00	
79% R.H.		1.28	1.26	1.96	1.60	1.50	0.48

[a] Initial sample was dried 3 days at 80° C.
[b] Sample was placed in desiccator containing Drierite after 1 week exposure to 79% R.H.
R.H., relative humidity over saturated salt solutions at 25° C.

HPLC. Type II showed no significant increase in the amount of known degradation products characteristic of this compound (Figazotto et al., 1991). In contrast, physical transformation of type I to type II can be observed microscopically (Fig. 6) when type I drug substance (Fig. 6a) is treated with a small amount of ethanol/water mixture and then evaporated to dryness; note the formation of needle-like particles (Fig. 6b). Similar behavior was found when type I was used in the preparation of suspension aerosol formulations (Fig. 6c); analysis of the resulting needles confirmed that they were in fact type II drug substance. The conversion appears accelerated by exposure to high humidity conditions, suggesting a critical humidity level must first be attained. Once started, the conversion process seems irreversible. However, isothermal calorimetry studies indicate that the kinetics of the I to II conversion are complex, and may be influenced by particle

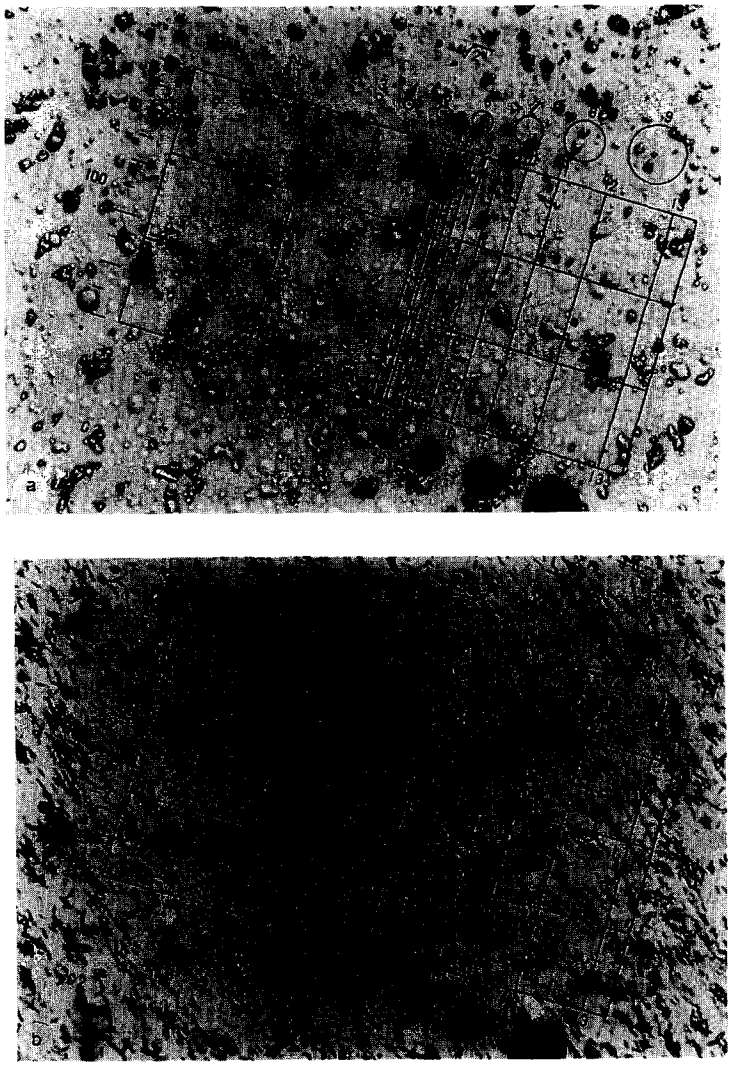

Fig. 6. Photomicrographs of SK&F 104353-Z_2: (a) initial suspension aerosol prepared from type I; (b) suspension aerosol after conversion of type I to type II; (c) type II drug substance resulting from treatment of type I with 50:50 ethanol/water. Note similarity of particle morphology in (b) and (c).

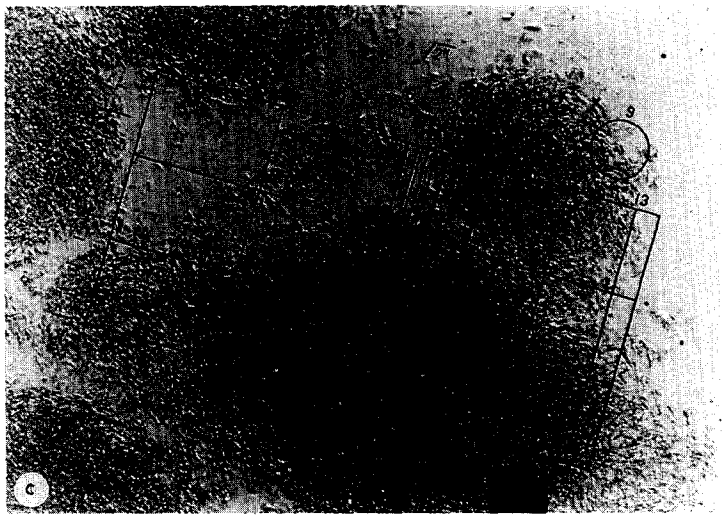

Fig. 6 (continued).

size, sample weight, and temperature, as well as humidity (Sokoloski et al., 1993). In the aforementioned ethanol slurry treatment studies, some lots of type I drug substance converted more readily than others, although all eventually could be induced to convert.

This lot-to-lot variability with respect to conversion can be evaluated more quantitatively using solution calorimetry. While this technique is most commonly applied to characterize differences in crystal structure due to polymorphism (Lindenbaum and McGraw, 1985), it has also been found useful in determining extent of crystallinity (Pikal et al., 1978). As shown in Table 2, type I samples which are not converted to type II yield heat of solution values virtually identical to their starting materials. Samples which are successfully converted give enthalpy of solution values on the order of 1–2 kcal/mol greater than unconverted lots. The solution calorimetry results correlate well with corresponding XRD and DSC data.

While polymorphic forms of other leukotriene antagonists have been reported (Ghodbane and McCauley, 1990), the XRD and DSC results in this case do not seem consistent with a true polymorphic conversion. The rapid conversion of I to II in the presence of high humidity raises the possibility of hydrate formation. However, the persistence of type II's low temperature DSC endotherms upon cooling and reheating is inconsistent with a hydrate, in which they would be expected to disappear after the initial heating. The similarity of the transitions when obtained in open as well as closed pans also argues against the existence of a stable hydrated form. Moreover, TGA and Karl Fischer determinations conducted on the same samples of types I and II

Table 2
Solution calorimetry data from 50:50 ethanol/water [a]

Run	Sample	Converted [b]	ΔH (kcal/mol)
A	initial		8.88
	final	yes	10.58
B	initial		8.35
	final	yes	10.38
C	initial		7.83
	final	yes	10.38
D	initial		8.56
	final	no	8.34
E	initial		9.71
	final	yes	12.15

[a] Runs A–D show the heats of solution for starting materials corresponding to different lots of drug substance (all type I) and the respective products produced by treating them with an ethanol-water slurry. Run E shows solution calorimetry data for another type I sample and its product produced by exposure to 40° C, 75% R.H storage (type II).

[b] Conversion of initial samples to type II was verified by XRD, DSC, and optical microscopy.

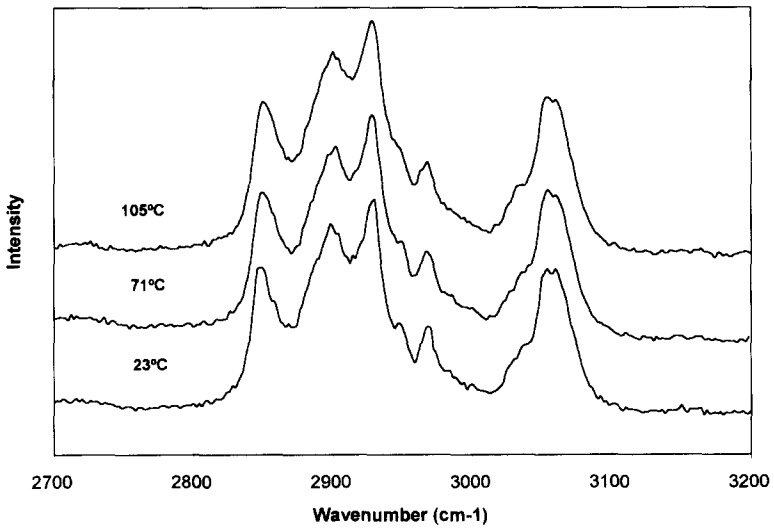

Fig. 7. FT-Raman spectra of SK&F 104353-Z_2, type I, at different temperatures.

showed no obvious differences in water content, which is on the order of 1.0% by weight; i.e., type II does not appear to be the result of permanently adsorbed excess moisture on the surface of type I. Note that a stoichiometric monohydrate of SK&F 104353-Z_2 would correspond to a weight loss on the order of 3.6%, a hemihydrate on the order of 1.8%. Also, a hydrate is expected to show a characteristic inflection in the TGA corresponding to dehydration; neither type I nor type II samples exhibit this behavior. Therefore, type II does not appear to be a hydrate of type I.

Examination of infrared and Raman spectra of the two types provides some further information regarding functional groups affected by the conversion process. The IR spectra (not shown) of

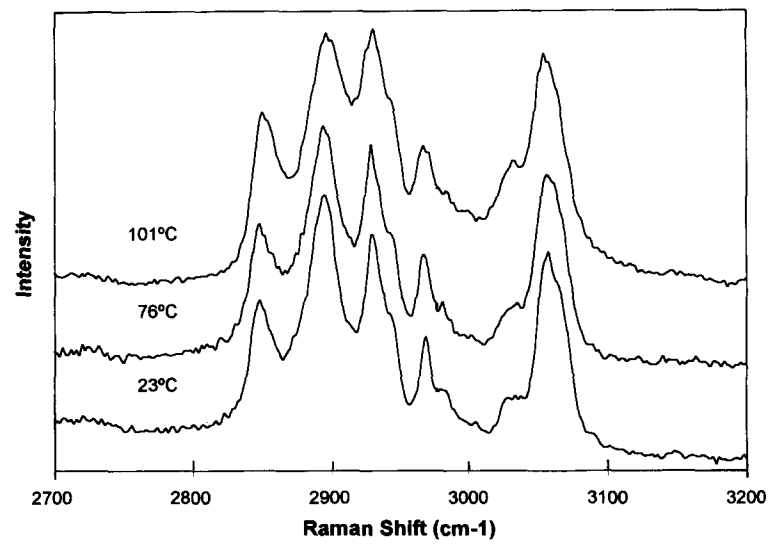

Fig. 8. FT-Raman spectra of SK&F 104353-Z_2, type II, at different temperatures.

Table 3
Location and assignment of SK&F 104353-Z_2 Raman bands

Frequency (cm^{-1})	Assignment
3055	aromatic C-H stretch
3030sh [a]	aromatic C-H stretch
2967	aliphatic C-H stretch
2932	symmetric CH_2 stretch
2901	antisymmetric CH_2 stretch
2855	antisymmetric CH_2 stretch
1605	aromatic ring vibration
1578	aromatic ring vibration

[a] sh, shoulder.

types I and II are quite similar; however, some differences can be more clearly seen when the spectrum of type I is subtracted from that of type II, particularly in the modes associated with mono- and disubstituted C-H deformation bands in the region of 900–675 cm^{-1} (Silverstein et al., 1974). A band at 712 cm^{-1}, which is assigned to the monosubstituted aromatic ring, appears to be most strongly associated with the conversion to higher crystallinity.

More obvious changes are apparent in the Raman spectra, with major peak frequencies and assignments summarized in Table 3. The most dramatic effects occur in the high frequency C-H stretching region. Fig. 7 and 8 show the temperature-dependent Raman spectra of types I and II. Two features are apparent from these figures. First, the room temperature Raman spectra are clearly different for the two types. Secondly, there are temperature-dependent effects observed only for type II, whereas the spectra for type I are temperature independent.

While changes at lower frequency are also observed, the most notable differences between the Raman spectra occur in the high-frequency C-H stretching region, from 2700 to 3200 cm^{-1}. This region includes vibrations from the aromatic moieties (3055, 3030 cm^{-1}, sh), the lone C-H stretch (2967 cm^{-1}), and from the methylene vibrations of the hydrophobic tail (8 CH_2) as well as the hydrophilic tail (2 CH_2). With respect to the aromatic stretching region, one can use the intensity ratio of the aromatic C-H stretch to the aromatic ring vibration as an internal standard. For both types I and II, the I_{3055}/I_{1605} ratio was 1.5, and did not change with temperature.

Attention thus focused on the aliphatic C-H stretches. The symmetric CH_2 stretch is known to be affected by the trans/gauche rotational isomerism of the hydrocarbon chain due to intramolecular Fermi resonance (Snyder et al., 1978, 1980) In particular, the symmetric stretch of highly ordered as well as completely disordered polyethylene chains appears as three bands, whose frequencies (at 2850, 2890, and 2929 cm^{-1}) do not change with phase but differ in relative intensities for disordered chains (i.e., a mixture of *trans* and *gauche* rotational isomers) vs ordered chains (all-*trans*). Note that the middle of the three bands is obscured by the strong antisymmetric CH_2 stretch which occurs nearby. However, the antisymmetric stretch at approx. 2900 cm^{-1} can couple to the torsional and librational motions of the alkane chain, and its width has been observed to depend on the mobility of the alkane chain (Zerbi et al., 1988).

The intensity ratios of both I_{2930}/I_{2850} and I_{2850}/I_{2890} have been used to characterize structure and phase transitions of hydrocarbon chains. First, I_{2930}/I_{2850} decreases for the transition from crystalline to liquid polyethylene (Snyder et al., 1982). In the case of SK&F 104353-Z2, this ratio stays approximately constant between the two types. Second, I_{2850}/I_{2890} decreases upon going from an ordered to a disordered chain (Snyder et al., 1978, 1980). In the present samples, where the actual ratio used is I_{2855}/I_{2890}, this ratio is on the order of 0.58 for type II and 0.73 for type I, suggesting an increased mobility in the type I state. A smaller decrease in the ratio is seen when type II is at temperatures above the observed DSC phase transition. It is thus possible that the methylene groups remain in a nearly all-*trans* conformation for all three phases, but are still more free to undergo torsional and librational oscillations in type I and in the high temperature phase of type II. Interestingly, hot-stage microscopy studies conducted on type II under crossed polars did not reveal any dramatic visual changes in this temperature range. However, a slight fading of birefringence was noted at approx. 70° C; this change was reversible upon cooling and reheating.

The temperature-dependent Raman spectra of

types I and II confirm that a phase change occurs for the high crystallinity type, but not for the low crystallinity type. No intensity changes were observed for type I, indicating that no conformational changes occur in the alkane chains with temperature. This clearly indicates that temperature alone does not provide sufficient mobility for a tranformation from type I to type II, By contrast, there is clear evidence of disordering at temperatures above the apparent DSC phase transitions of type II. Once such a transition occurs, no further changes with temperature are observed (spectra were recorded up to 150° C but are not shown). The major change in the higer temperature form appears as a lowering in the intensity of the 2899 cm^{-1} band, which decreases to a value that is still higher than that observed for the low crystalline (type I) form.

An X-ray structural determination carried out on the crystalline racemate of SK&F 104353 (SK &F 103944) indicates that hydrophobic and hydrophilic groups are segregated by the molecular packing, with the lipophilic chains packed in a head to tail arrangement (Eggleston et al., 1990). We postulate that exposure of type I to moisture allows some mobility within the lipophilic 'tail' regions; reorientation of the tail could conceivably facilitate growth of small, isolated crystals already present in I, leading to a product of higher crystallinity. The precise significance of the low-enthalpy, weak DSC transitions in type II remains to be determined; however, their presence appears to be indicative of the increased crystalline character. It is also of interest to note that low-enthalpy solid-solid transitions have been observed in some paraffins, which may be relevant to the present compounds (Lourdin et al., 1992). Further studies utilizing spectroscopy and/or microscopy as a function of temperature are expected to provide additional insight into their origin in the leukotriene antagonists.

From a formulation standpoint, type I is clearly problematic to work with, since it can readily convert to II and the conversion cannot be easily suppressed or controlled. This physical instability is a particular concern for aerosol formulation, wherein particle size and morphology must be controlled to achieve desired therapeutic behavior. Crystal growth in MDI formulations is undesirable, as it decreases the amount of respirable drug available, and can also lead to unsatisfactory performance of the inhaler device (Dalby et al., 1991). Suspension aerosol formulations prepared with type I were found to be unsatisfactory in this regard, while MDIs prepared with micronized type II appear to be physically stable, even when stored under high humidity conditions, making this form preferable for formulation development.

However, attempts to produce type II on a practical scale were not particularly successful; the final precipitation step appears to be extremely sensitive to the amount of moisture present. This suggests that the role of water may be that of a transient solubilizing agent, which allows type I to dissolve and then recrystallize out as the more highly crystalline type II species. It also seems clear while water facilitates conversion of type I to type II, the latter does not represent a hydrated species and is not different chemically from type I starting material.

A previous report dealing with a structurally similar leukotriene antagonist (Vadas et al., 1991) suggests that this class of compounds can exhibit unusual solid-state behavior. It was speculated that the observed thermal and microscopic behavior might stem from the amphiphilic nature and surface activity of these molecules, which allows them to exist in liquid crystalline phases. However, in the present case, the conversion of type I to type II appears to be unrelated to liquid crystal characteristics; rather, the DSC and hot-stage polarized light microscopy studies indicate that a solid-solid phase transition occurs below 100° C, which appears to be correlated with increased crystallinity. One unusual feature is its persistence, i.e., this transition does not disappear upon repeated annealing, as would be expected for other partially crystalline systems.

4. Conclusions

The growing importance of leukotriene antagonist compounds in pharmaceutical development will require thorough preformulation studies us-

ing a variety of techniques. Such early-stage studies are a prerequiste for better understanding how their structural features impact on the physical stability of these compounds in dosage forms. Calorimetric methods and Raman spectroscopy in particular may be useful in monitoring changes in the solid-state behavior of this class of compounds.

Acknowledgements

We wish to acknowledge the expert technical assistance of Etha McDowell, Al Jarmas, and Gary Zuber. We also thank Drs Kerry Gombatz and Vance Novack for providing helpful information on the preparation of SK&F 104353 and its salts.

References

Dalby, R.N., Phillips, E.M. and Byron, P.M., Determination of drug solubility in aerosol propellants. *Pharm. Res.*, 8 (1991) 1206–1209.

Eggleston, D.S. Hall, R.F. and Gleason, J.G., Structures of leukotriene antagonists: racemic 2-hydroxy-3-[2-(8-phenyloctyl)phenyl]-4-thiaheptanedioic acid, SK&F 103944. *Acta Crystallogr.*, C46 (1990) 1244–1248.

Figazotto, A.C., Renfrow, R.A., McLoughlin, M., O'Reilly, M. and Rossi, T.M., Degradation chemistry of two leukotriene antagonists: Unexpected difference in the reactivities of the sulfoxide intermediates. *Pharm. Res.*, 8 (1991) S–33.

Flisak, J.R., Gombatz, K.J., Holmes, M.M., Jarmas, A.A., Lantos, I. Mendelson W.L., Novack, V.J., Remich, J.J. and Snyder, L., A practical, enantioselective synthesis of SK&F 104353. *J. Org. Chem.*, 58 (1993) 6247–6254.

Ghodbane, S. and McCauley, J.A., Study of the polymorphism of 3-((3-(2-(7-chloro-2-quinolinyl)-(*E*)-ethenyl)phenyl)(3-dimethylamino-3-oxopropyl)thio)methyl)thio)propanoic acid (MK571) by DSC, TG, XPRD, and solubility measurements. *Int. J. Pharm.*, 59 (1990) 281–286.

Gleason, J.G., Hall, R.F., Perchonock, C.D., Erhard, K.F., Frazee, J.S., Ku, T.W., Kondrad, K., McCarthy, M.E., Mong, S., Crooke, S.T., Chi-Rosso, G., Wasserman, M.A., Torphy, T.J., Muccitelli, R.M., Hay, D.W., Tucker, S.S. and Vickery-Clark, L., High affinity leukotriene receptor antagonists. Synthesis and pharmacological characterization of 2-hydroxy-3-[(2-carboxyethyl)thio-3-[2-(8-phenyloctyl)phenylpropanoic acid. *J. Med. Chem.*, 30 (1987) 959–961.

Lindenbaum, S. and McGraw, S.E., The identification and characterization of polymorphism in drug solids by solution calorimetry. *Pharm. Manuf.*, Jan. (1985) 27–30.

Lourdin, D., Roux, A.H., Grolier, J.-P.E. and Buisine, J.-M., Thermobarometric and differential scanning calorimetric study of the polymorphism of some even and odd paraffins (C26, C27, C40, C60). *Thermochim. Acta*, 204 (1992) 99–110.

Pikal, M.J., Lukes, A.L., Lang, J.E. and Gains, K.E., Quantitative crystallinity determinations for β-antibiotics by solution calorimetry. *J. Pharm. Sci.*, 67 (1978) 767–773.

Robuschi, M., Riva, E., Fuccella, L.M., Vida, E., Barnabe, R., Rossi, M., Gambaro, G., Spagnotto, S. and Bianco, S., Prevention of exercise-induced bronchoconstriction of a new leukotriene antagonist (SK&F 104353). *Am. Rev. Respir. Dis.*, 145 (1992) 1285–1288.

Silverstein, R.M., Bassler, G.C. and Morrill, T.C., *Spectrometric Identification of Organic Compounds*, 3rd Edn, Wiley, New York, 1974.

Snyder, R.G., Hsu, S.L. and Krimm, S., Vibrational spectra in the carbon-hydrogen stretching region of the polymethylene chain. *Spectrochim. Acta*, 34A (1978) 395–406.

Snyder, R.G., Scherer, J.R. and Gaber, B.P., Effects of chain packing and chain mobility on the Raman spectra of biomembranes. *Biochim. Biophys. Acta*, 601 (1980) 47–53.

Snyder, R.G., Strauss, H.L. and Elliger, C.A., C-H stretching modes and the structure of *n*-alkyl chains. 1. Long, disordered chains. *J. Phys. Chem.*, 86 (1982) 5145–5150.

Sokoloski, T.D., Morris, M.E., Randall, C.S., Duddu, S., Milosovich, S.M. and Patel, K.H., Application of thermal analyses to study drug-water interactions: I. Transitions in leukotriene antagonists. *48th Annual Calorimetry Conference*, July 1993.

Vadas, E.B., Toma, P. and Zografi, G., Solid-state phase transitions initiated by water vapor sorption of crystalline L-660,711, a leukotriene D4 receptor antagonist. *Pharm. Res.*, 8 (1991) 148–155.

Zerbi, G., Roncone, P., Longhi, G. and Wunder, S.L., Molecular flexibility of polymethylene molecules: A Raman spectroscopic study. *J. Chem. Phys.*, 89 (1988) 166–173.